A model based on transient optical depletion of causal impurity molecules successfully accounts for the observed efficiency of luminescence quenching. Although these experimental and theoretical results prove the applicability of the present method to a certain extent, this technique must still be examined by further extensive studies that include many luminescent materials of various origins. From a practical viewpoint, however, it seems advisable to simply try pulsed excitation in place of the conventional cw method. It must be noted in conclusion, however, that the present method is by no means applicable to a case in which luminescence originates from the sample molecule itself.

ACKNOWLEDGMENTS

The authors are grateful to Drs. Y. Nishimura and M. Tanokura for supplying the samples. Thanks are also due to Mr. T. Yamamoto for his help in the sample preparation.

1. T. Tahara, H. Hamaguchi, and M. Tasumi, J. Phys. Chem. in press.
2. T. Tahara, H. Hamaguchi, and M. Tasumi, Chem. Lett. **1987,** 1219.
3. J. Matsuzaki, H. Hotoda, M. Sekine, T. Hata, S. Higuchi, Y. Nishimura, and M. Tsuboi, Tetrahedron **42,** 501 (1986).
4. Y. Ogura and M. Tanokura, J. Biochem. **95,** 19 (1984).
5. Y. Nishimura, private communication.
6. B. A. Seaton, J. F. Head, R. C. Lord, and G. A. Petsko, Biochemistry **22,** 973 (1983).
7. H. Hamaguchi, Chem. Phys. Lett. **126,** 185 (1986).

High-Repetition-Rate Excimer-Based UV Laser Excitation Source Avoids Saturation in Resonance Raman Measurements of Tyrosinate and Pyrene

COLLEEN M. JONES, VALENTINO L. DEVITO, PAUL A. HARMON, and SANFORD A. ASHER*

Department of Chemistry, University of Pittsburgh, Pittsburgh, Pennsylvania 15260

UV resonance Raman excitation using low-duty-cycle pulsed lasers such as the Nd:YAG can result in photophysical processes that interfere with Raman spectral studies of ground-state species due to the high incident laser energy fluxes. Depletion of the ground state occurs due to optical absorption and due to the population of intermediate levels which have lifetimes comparable to or longer than the excitation pulse width. In addition, formation of photochemical intermediates can occur. For example, excitation in resonance with the tyrosinate L_a electronic transition (~240 nm) results in formation of tyrosyl radicals which deplete the concentration of ground-state tyrosinate molecules; as a result, decreased resonance Raman intensities are observed for vibrational modes of ground-state tyrosinate. For pyrene, excitation in resonance with the S_4 electronic transition results in population of the long-lived S_1 state via rapid internal conversion. This long-lived state bottlenecks relaxation back to the ground state, thus causing saturation of the ground-state pyrene Raman intensities. Given similar incident *average* laser powers and focusing conditions, higher-duty-cycle lasers result in decreased saturation. A comparison between a 20-Hz Nd:YAG and a 200-Hz excimer laser-based UV Raman excitation source demonstrates superiority of the excimer in avoiding both Raman saturation and interferences from photochemical transients. For the identical energy flux per pulse, the accompanying tenfold increase in *average* energy flux for the excimer, over the YAG, results in a dramatic improvement in the spectral signal-to-noise ratios. We report the first measurement of the absolute resonance Raman cross section of pyrene within the S_4 transition. The Raman cross section of 48 barns/str measured for the 1632-cm^{-1} vibration with 240-nm excitation is the largest observed to date.

Index Headings: Resonance Raman spectroscopy; UV laser sources; Raman saturation of tyrosinate and pyrene.

Received 4 August 1987.

* Author to whom correspondence should be sent.

INTRODUCTION

The recent development of UV laser excitation sources has permitted the extension of resonance Raman spectroscopy to molecules with electronic transitions in the near-, mid-, and far-UV spectral regions.[1-7] The importance of these studies is (1) that they advance the fundamental understanding of molecular structure and dynamics and (2) that UV resonance Raman spectroscopy can be applied to important problems in biophysical, analytical, and physical chemistry. It is now possible to resonantly excite Raman spectra within the $\pi \rightarrow \pi^*$ transitions of molecules as small as ethylene,[6] as well as within the strong absorption bands of larger molecules such as aromatic amino acids[8-11] and nucleic acids[12] and the absorption bands of polycyclic aromatic hydrocarbons.[5,13-15] For any Raman study it is crucial to determine the Raman cross sections, since the resulting intensity information can be used to determine the concentrations of species of interest,[5] as well as to monitor molecular environment[9] and to examine molecular excited-state distortions.[16,17] This factor has led to numerous recent studies of resonance Raman cross section excitation profiles.[7,9,11,16] For example, the individual aromatic amino acid excitation profiles can provide the information required to selectively enhance particular aromatic amino acid residues in proteins.[8,9,11,18]

The excitation wavelengths required to spectroscopically probe UV molecular transitions can be generated with the use of nonlinear optical frequency conversion

0003-7028/87/4108-1268$2.00/0

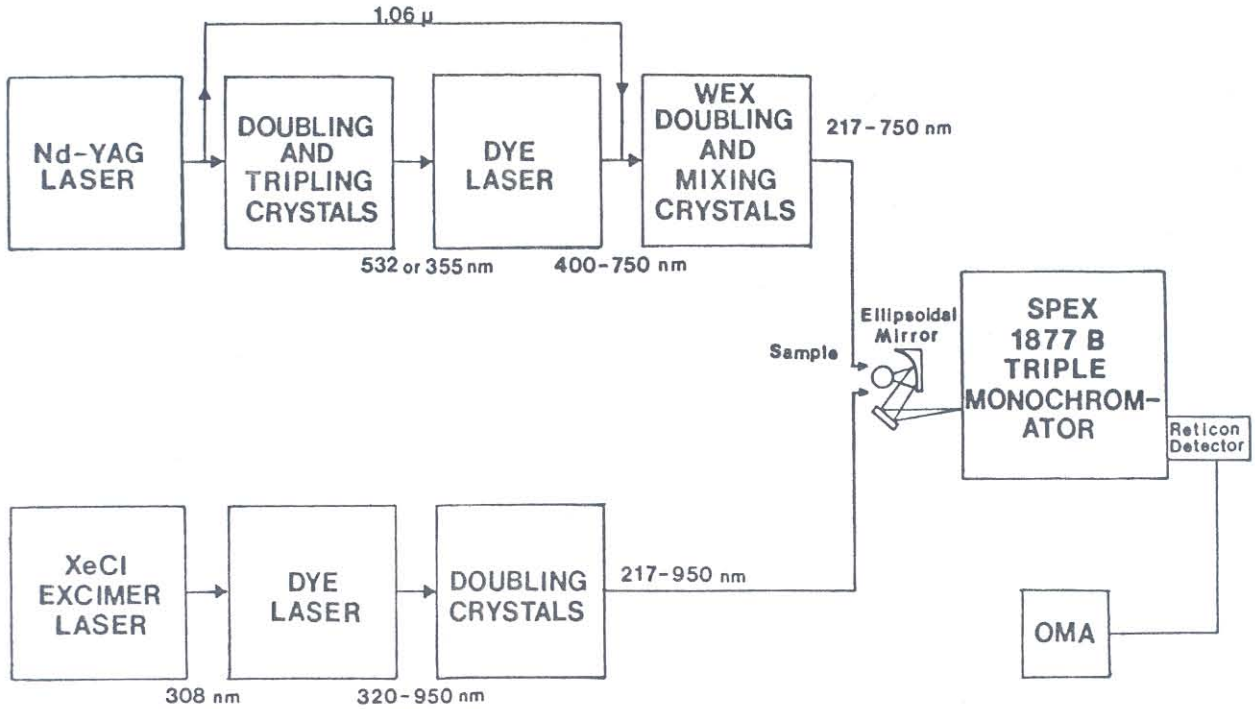

FIG. 1. Block diagram of the Nd:YAG and XeCl excimer UV resonance Raman spectrometers.

techniques.[19] Pulsed laser sources such as the Nd:YAG and excimer lasers provide the high electric field strengths necessary for efficient frequency conversion. Wavelengths down to 217 nm may be obtained from these systems with the use of nonlinear crystals to modulate the fundamental and dye laser frequencies.[1] Unfortunately, the high power fluxes (W/cm^2) and pulse energies associated with these pulsed UV excitation sources can induce processes that complicate resonance Raman spectral measurements.[20] In addition to resonance Raman scattering, excitation within an electronic absorption band results in significant population of the resonant excited state, which can lead to sample photochemistry. Saturation of the Raman intensities will also occur at high incident energy excitation if significant depletion of the ground-state population occurs during the leading edge of the laser pulse; fewer ground-state analyte molecules become available for Raman scattering during the trailing edge of the pulse. Experimentally, the ratios of the intensities of the analyte Raman bands to those of the internal standard bands will decrease with an increase in incident average laser power and tighter focusing. Recent UV resonance Raman studies of tyrosine and of tyrosinate were plagued by both saturation and phototransient formation, which resulted in the mistaken assignment of photochemical intermediate bands as ground-state vibrations.[8,10] Raman saturation induced by the high peak pulse powers and the high pulse energies of Nd:YAG lasers complicates measurements of the excitation profiles of the aromatic amino acids and has effectively prevented quantitative measurements of the excitation profiles of tryptophan and pyrene.[9,11,15]

In this study we demonstrate that use of a lower-peak-pulse-power, lower-pulse-energy 200-Hz excimer laser avoids saturation for tyrosinate and pyrene. We compare the Raman spectral measurements of pyrene and tyrosinate, using the Nd:YAG and excimer excitation sources under conditions of similar incident average laser power flux per pulse, and find dramatic improvements in the signal-to-noise ratios with the excimer-based system; for the same power or energy flux per pulse, the 200-Hz excimer permits the use of ten times the *average* power or energy flux.

EXPERIMENTAL

Figure 1 shows the block diagram of the laser excitation sources and the spectrometer used. The 308-nm fundamental of a 200-Hz Lambda-Physik Model EMG 103 MSC XeCl excimer laser was used to pump a Lambda-Physik Model FL 3002 dye laser, which was frequency-doubled to generate the UV excitation light used in this study.

The Nd:YAG UV laser excitation source and the Raman spectrometer have been described previously.[1] The frequency-doubled fundamental of a Quanta-Ray DCR-2A laser operated at 20 Hz was used to pump a Quanta-Ray Model PDL-1 dye laser. The dye laser output was frequency doubled and mixed with the IR fundamental to obtain the UV excitation frequency used to excite the samples. The same monochromator and detection system was used for both the YAG and excimer experiments. The 0.1 mM solutions of pyrene (Chem Services, West Chester, PA) in acetonitrile were recirculated through a 1.0-mm-i.d. suprasil quartz sampling capillary. The 5 mM tyrosinate (Sigma) aqueous solutions at pH = 12 were pumped through a dye laser nozzle; the resulting thin film of solution was excited with the focused laser beam, and the ~5-mL solutions were recirculated during each spectral measurement. The Raman scattered light was collected at ninety degrees and focused onto the entrance slit of a Spex Triplemate monochromator by

an ellipsoidal mirror. The 1200 groove/mm grating used in the spectrograph stage of the Triplemate gave a spectral bandpass of ~24 cm^{-1} at 240 nm for our spectrograph slit width of 200 μm. A crystalline quartz polarizing wedge was used to eliminate any polarization bias of the monochromator. An EG&G PAR Model 1420 Reticon detector and an optical multichannel analyzer (PAR OMA II) were used to acquire the data. Typical scan times were five minutes. The absolute Raman cross-section values were obtained after the Raman scattering intensities were corrected for monochromator efficiency. The Raman cross sections for the internal standard bands were obtained from the measurements of Dudik *et al.*[7] Self-absorption corrections were neglected; the short pathlength of the sample film (0.1 mm) used to acquire the tyrosinate data results in minimal self-absorption. The pyrene intensities were not corrected for self-absorption, since the Raman scattered frequencies occur in spectral regions where the molar absorptivities are essentially identical for the pyrene and internal standard Raman bands.

The incident pulse energy flux was varied either by adjusting the focusing lens which directs the laser beam into sampling capillary or jet or by using neutral-density filters to attenuate the incident average laser power. The energy flux at the sample was calculated from measurements of the laser beam width at the sample with different focusing conditions. The YAG beam width was determined to be ~110 μm when focused by a 25-cm-focal-length lens directly into the sample and ~210 and 410 μm when defocused 15 and 45 mm past the sample, respectively. The excimer beam diameters at the sample were ~90, 210, and 450 μm when the beam was focused in the sample and focused 15 and 45 mm past the sample, respectively. The beam diameters derive from measurements over numerous pulses and therefore represent an upper limit for the focused beam diameters; we will overestimate the spot size of a single pulse if spatial beam jitter is significant. Furthermore, the spatial mode profile of the excimer is irregular and deviates from the cylindrical beam shape assumed in our calculations. The pulse widths used in the pulse energy flux calculations were measured as 6 ns for the YAG and 16 ns for the excimer laser. The actual temporal shape of the Q-switched YAG excitation pulse is an envelope of short ps pulses which derive from different longitudinal modes of the cavity. Since this envelope varies between pulses, and since we average over numerous pulses in our measurements, we ignore the YAG temporal fine structure but recognize that the actual instantaneous peak energy fluxes can be higher than those we calculate. The energy flux depends inversely upon both the square of the beam diameter and the pulse length. We estimate that our calculated energy flux could be in error by as much as 50% when we compare the YAG to the excimer; however, the relative energy fluxes within a series of experiments using only the YAG, or experiments using only the excimer, are likely to be accurate to better than 20%.

RESULTS AND DISCUSSION

Tyrosinate. We previously described the phototransient formation and Raman saturation phenomena that occur for tyrosinate when high-peak-pulse-power UV excitation occurs within the tyrosinate $S_2(L_a)$ $\pi \rightarrow \pi^*$ electronic transition.[20] Tyrosinate saturation was shown to increase with increasing molar absorptivity[11,20] and was most severe with excitation at the L_a absorption maximum (240 nm). Tyrosinate is easily oxidized and probably photoionizes with excitation into S_2 via a charge transfer to the solvent.[21] Figure 2 shows the resonance Raman spectra of tyrosinate excited at the S_2 absorption maximum (240 nm) with the use of both the excimer and Nd:YAG lasers. Ground-state tyrosinate vibrations occur at 831, 852, 1174, 1207, and 1599 cm^{-1}. At high incident energy fluxes, new vibrational bands are observed in the Raman spectra that derive from tyrosyl radical species that form as a result of a monophotonic photoionization. Resonance Raman scattering from the tyrosyl radical results in the appearance of new bands at 810, 975, 1160, 1402, 1510, and 1565 cm^{-1} with 245 nm excitation. The transient bands at 810, 975, and 1160 cm^{-1} are not apparent in Fig. 2, either because they strongly overlap the ground-state tyrosinate vibrational bands or because of their weak intensities.

The spectra are arranged so that the data acquired under similar experimental conditions (i.e., same focusing and incident average laser power) with the Nd:YAG and excimer lasers are adjacent to one another, to facilitate direct comparison (also see Table I). The spectra are arranged in order of decreasing energy flux within a particular column. Note that, given the same focusing and incident average laser power, a higher energy flux is delivered to the sample with the use of the YAG excitation source, because of the lower pulse repetition rate relative to that of the excimer source. Saturation is clearly evident with both excitation sources; the ratios of the tyrosinate band intensities relative to the internal standard band intensity increase with decreasing incident energy flux.

It is obvious, comparing the YAG and excimer spectra, that the higher energy fluxes of the YAG consistently result in greater saturation and phototransient formation. Figure 2A (YAG), which was acquired with the use of the highest energy flux, shows severe saturation of the tyrosinate ground-state vibrational intensities. Intense bands are observed from tyrosyl radical. Tyrosyl radical formation removes molecules from the ground state, causing decreased resonance Raman scattering from the tyrosinate ground-state species. However, as the incident energy flux of the YAG is decreased, the intensities of the photochemical transient bands decrease, until these vibrations are no longer observed [see Fig. 2D (YAG)]; while, at the same time, the relative intensity ratios of the ground-state tyrosinate bands to the internal standard intensity increase.

For the excimer-excited spectra, saturation is obvious only for the spectrum excited at the highest energy flux [i.e., Fig. 2A (EX)]. Saturation is less evident in Fig. 2B, C, and D (EX), which were obtained under low energy flux conditions; the measured intensity ratios of the 1174 and 1599 cm^{-1} tyrosinate ground-state vibrations relative to the internal standard band show only slight changes with lower energy flux. The dependence of these intensity ratios upon incident energy flux is shown in Fig. 3. As expected, the ratio of intensities of tyrosinate to the internal standard decreases as the integrated power flux

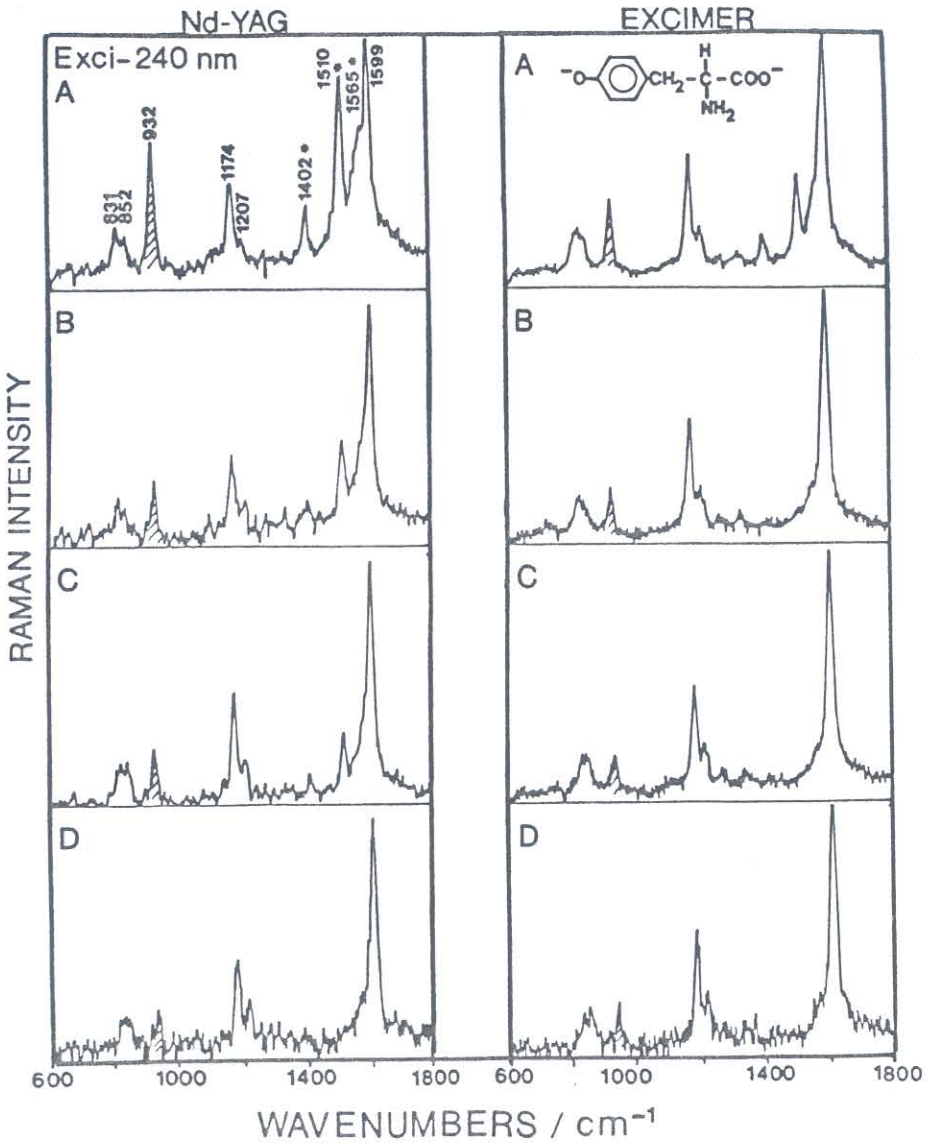

FIG. 2. UV resonance Raman spectra of 5 mM aqueous solutions (pH = 12) of tyrosinate excited at 240 nm with the use of Nd:YAG and excimer laser sources. Experimental conditions for spectra A–D are reported in Table I. The 932 cm^{-1} perchlorate (1 M) internal intensity standard band is shaded, and tyrosyl radical bands are starred in the figure.

(pulse energy flux) increases. Further, the intensity ratio for the 1510 cm^{-1} tyrosyl radical band shows an approximately linear increase as the pulse energy increases.

Previously, we derived[11,20] a relationship for the dependence of saturation of Raman intensities upon incident power flux for the simple model where a photon may either be absorbed or give rise to resonance Raman scattering. Absorption transfers a ground-state molecule to an intermediate state, which may be either a molecular excited-state or a photochemical product. This excited-state or photochemical product may also show Raman bands, provided that they can be resolved from that of the ground-state analyte. The model assumes that no relaxation back to ground state occurs during a laser pulse and that the sample solution is replenished between pulses.

For low pulse energies, the relative intensities of the ground-state analyte Raman bands, compared with the intensities of the photochemically inactive internal standard bands, will decrease linearly with increasing pulse energy. The slope of this decrease is proportional to the absorption cross section. The Raman intensity of any photochemical intermediate will increase with a slope which is also proportional to the absorption cross section. The ratio of the slopes of the ground-state species and the photochemical trnasient is directly proportional to the ratio of their Raman cross sections:

$$S_p \approx \frac{\sigma_p P_0}{\sigma_c C_0}\left[1 - \frac{\sigma_A J_0}{2}\right] \quad (1)$$

$$S_T = \frac{\sigma_T P_0 \sigma_A J_0}{2\sigma_c C_0} \quad (2)$$

where S_P and S_T are the relative intensities of the ground-state species and the transient compared with that of the internal standard, respectively, while σ_P, and σ_T, and σ_c are the Raman cross sections of the ground-state analyte, the transient, and the internal standard, respectively. σ_A is the absorption cross section of the ground-

TABLE I. Experimental conditions.

Spectrum	Nd:YAG Power[a] flux	Nd:YAG Energy[b] flux	Nd:YAG Incident average power (mW)	Nd:YAG Focus[c]	Excimer Power[a] flux	Excimer Energy[b] flux	Excimer Incident average power (mW)	Excimer Focus[c]
Tyrosinate experimental conditions								
Fig. 2A	800	4800	9	F	55	880	11	F
B	200	1200	2	F	10	160	2	F
C	200	1200	8	D2	6	96	7	D2
D	50	300	2	D2	2	32	2	D2
Pyrene experimental conditions								
Fig. 4A	>70	>420	3	D1	>2	>32	2	D1
B	70	420	3	D2	2	32	2	D2
C	10	76	2	D3	0.5	6	2	D3
D	3	19	0.5	D3	0.1	1.6	0.5	D3
E	1	4	0.2	D3	0.04	0.3	0.2	D3

[a] Mega-Watts/cm^2·pulse.
[b] Millijoules/cm^2·pulse.
[c] Using a 25-cm-focal-length lens, we measure beam diameters of 110 μm (90 μm), 210 μm (210 μm), and 410 μm (450 μm) for the Nd:YAG (excimer) when the beam was focused at the sample (F), focused less than 15 mm past the sample (D1), diffusely focused 15 mm past the sample (D2), or very diffusely focused 45 mm past the sample (D3).

state analyte, while P_0 and C_0 are concentrations of the analyte and internal standard, respectively. J_0 is the integrated power flux or pulse energy.

The more general model for saturation must include the common situation where excited-state relaxation takes place during the laser pulse. In this case the expression for saturation becomes more complex, and the degree of saturation depends intimately upon both the power flux and the pulse length. For temporally complex laser pulse shapes the saturation can only be calculated by integration of the kinetic expressions over the pulse shape. We will describe these dependences in detail in the near future.[22] However, the saturation phenomena observed here are completely described by the simple model, since negligible ground-state recovery occurs within the laser pulse, due to the long lifetimes of the intermediate states of tyrosinate and pyrene (*vide infra*).

The data indicate that in the wavelength region studied here tyrosinate saturation derives primarily from tyrosyl radical formation. It should be noted, however, that although Fig. 2C, B, and A (YAG) show increasing saturation, no accompanying increase is evident for the 1510 cm^{-1} tyrosyl radical band intensity relative to the internal standard intensity at the highest energy fluxes. This suggests that at high energy fluxes the tyrosyl radical concentration remains relatively constant as the excitation energy flux increases—a result which is inconsistent with a simple saturation mechanism where an increasing degree of saturation would be accompanied by the formation of more tyrosyl radicals. Apparently the tyrosyl radical Raman intensities also saturate at these higher energy fluxes, due to other photochemical reactions. Because of the large enhancements shown by tyrosyl radical with 240 nm excitation, it is clear that a strong absorption must occur at this wavelength. Population of radical excited states, or possibly formation of a second photochemical intermediate at higher energy fluxes, may deplete the tyrosyl radical concentration.

Saturation has a dramatic impact on the measured relative intensities. For example, in the YAG data, a factor-of-four change occurs in the relative intensities of the tyrosinate to the internal standard. The lack of saturation in excimer spectra of Fig. 2B, C, and D (EX) allows us to accurately measure the absolute Raman cross section of the 1599 cm^{-1} tyrosinate vibration as 0.44 barns/str (1 barn = 10^{-24} cm^2/molc) for 240 nm excitation. (We estimate a ±15% error present in the absolute Raman cross sections that derives primarily from experimental uncertainties in our peak height measurements at the lowest laser powers.) A previous measurement of this cross section, which attempted to minimize saturation with the YAG laser system, gave a value which was ~25% lower.[9]

Pyrene. The photophysical mechanism for pyrene saturation differs from that for tyrosinate saturation. We demonstrated that excitation into pyrene's S_4 excited electronic transition results in absorption followed by rapid internal conversion to the S_1 excited electronic

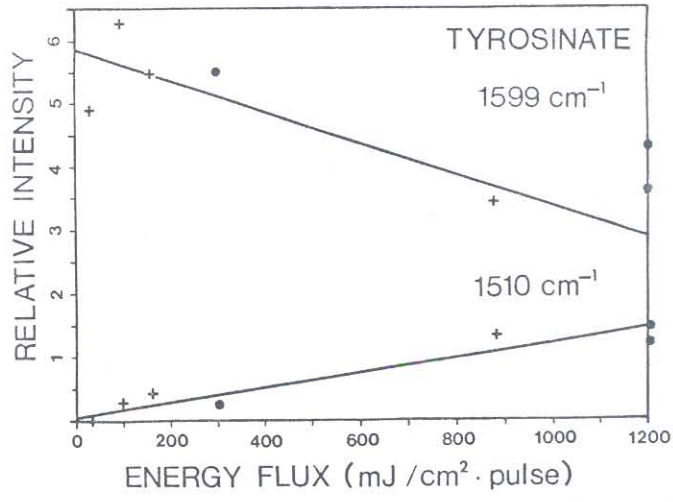

FIG. 3. The pulse energy flux dependence of the observed ratios of the 1599 cm^{-1} tyrosinate ground-state band intensity and the 1510 cm^{-1} tyrosyl radical band intensity relative to the 932 cm^{-1} ClO_4^- internal standard band intensity. The intensity data are from Fig. 2, while the energy flux data are listed in Table I. Note that the highest energy flux data from Fig. 2A (YAG) are not included, since this energy flux exceeds the values where a linear dependence occurs. Excimer (+), YAG (●). The solid lines show the least-squares fit to the initial slope.

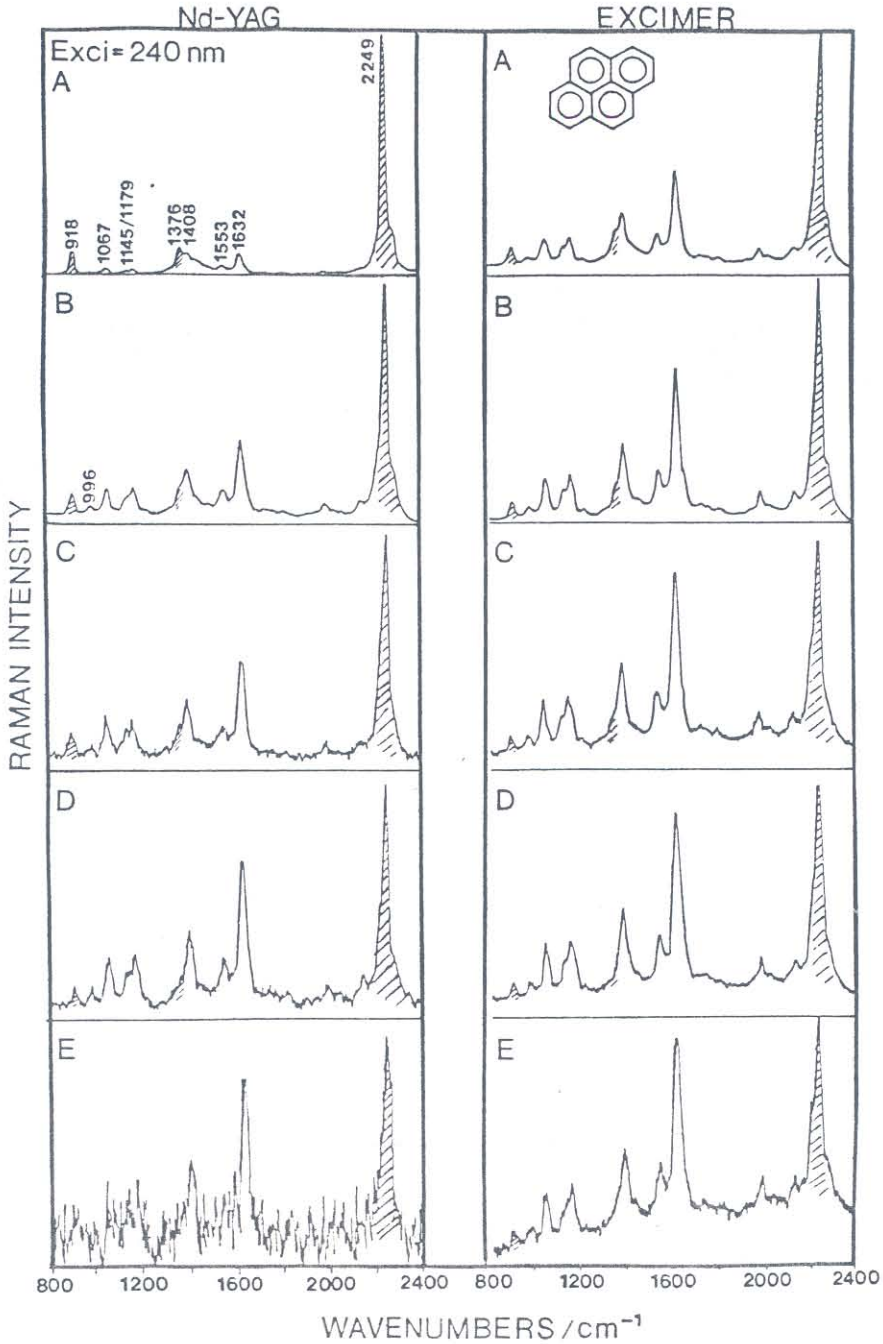

FIG. 4. UV resonance Raman spectra of 0.1 mM pyrene in acetonitrile excited at 240 nm with the use of both the Nd:YAG and excimer laser sources. Experimental conditions for spectra A–E are reported in Table I. The 918, 1376, and 2249 cm^{-1} acetonitrile internal intensity standard vibrations are shaded in the figure.

state for pyrene in solution.[15] Population of this long-lived (~300 ns) first excited singlet state results in saturation of pyrene vibrational intensities, since relaxation back to the ground electronic state is bottlenecked during the laser excitation pulse.[23,24]

Resonance Raman spectra of pyrene excited at the S_4 absorption maximum (240 nm) with the use of both YAG and excimer excitations are shown in Fig. 4. All bands observed derive from resonance Raman scattering from ground-state pyrene molecules. Pyrene in-plane ring vibrations resonantly enhanced with excitation in S_4 appear at 1067, 1145, 1179, 1408, 1553, and 1632 cm^{-1}.

The pyrene spectra obtained under similar experimental conditions (i.e., incident average laser power and focusing) with the YAG and excimer lasers are adjacent to one another in Fig. 4. The pulse energy fluxes and experimental conditions are given in the lower portion of Table I. As for tyrosinate, the high energy flux per pulse of the UV laser sources results in saturation of the pyrene Raman intensities; this is manifested as an increase in the ratios of the intensities of the pyrene bands relative to that of the internal standard band as the incident energy flux decreases. This dependence is graphically displayed in Fig. 5. The higher incident energy flux delivered by the YAG once again results in greater pyrene saturation than does the excimer laser

source. Figure 4 spectra C, D, and E (EX), which were acquired under low energy flux conditions, exhibit little saturation; thus, reliable absolute Raman scattering cross sections of the pyrene vibrations can be obtained. The 1632 cm^{-1} pyrene mode, the vibration most strongly enhanced with excitation in resonance with the S_4 electronic transition, has an absolute Raman cross section of 48 barns/str at 240 nm excitation. To our knowledge, this is the largest absolute resonance Raman cross section reported to date. This cross section is ~ 10 times larger than that which would have been incorrectly calculated with the use of the saturated Raman spectra obtained with the YAG excitation source under the highest energy flux.

The dependence of saturation on the pulse energy flux displayed in Figs. 3 and 5 indicates that, as expected, tyrosinate remains linear over a larger energy flux region than does pyrene, due to its eight fold smaller value of σ_A. The agreement between the observed slope ratio (3.8) and the ratio (3.6) calculated by the use of the measured values for σ_p, σ_c, P_0, and C_0 strongly supports our model for saturation for the lower energy flux conditions.

Examination of Figs. 2 and 4, as well as Table I, clearly shows that, under similar energy flux conditions, Raman spectra obtained with the excimer consistently show higher signal-to-noise ratios than those obtained with the YAG. This improvement in the spectral signal-to-noise ratio for the excimer (compared with the YAG) occurs because, for the identical energy flux per pulse, the excimer delivers ten times more average energy flux per second that does the YAG, due to its tenfold higher repetition rate. This translates directly into a tenfold increase in the measured Raman intensities. Both lasers, if tightly focused, can easily deliver energy fluxes which cause significant saturation of the Raman intensities. These energy fluxes can be attenuated either by defocusing the beam or by attenuating the incident intensity. The important parameter is the effective average energy that can be imaged into the sample volume that is collected by the sampling optics and transferred into the spectrometer. Obviously, the excimer permits a tenfold increase in the average Raman intensity for the same incident energy flux per pulse. The advantage of the excimer will be even greater in situations where relaxation can repopulate the ground state during the 16-ns interval of the excimer pulse. In this case the 2.6-fold increase in the excimer pulse duration, compared with that of the YAG, will result in additional Raman scattering from ground-state molecules.

The tenfold increase in energy imaged into the sample volume, which results in a tenfold increase in the Raman intensity, translates into an increase in the signal-to-noise ratios. For the high signal limit where shot-noise dominates, the tenfold intensity increase corresponds to a signal-to-noise increase of 3.2. In contrast, for the typical UV Raman measurement, where the noise derives directly from the Reticon detector and is independent of signal, the signal-to-noise will improve by a factor of ten. An upper limit exists for the maximum pulse energy flux which can be used to study ground-state species due to saturation, photochemical transient formation, and nonlinear optical processes such as stimulated Raman scattering. Because of this limit, the excimer laser source, compared with the YAG, invariably leads to higher sensitivity and signal-to-noise ratios.

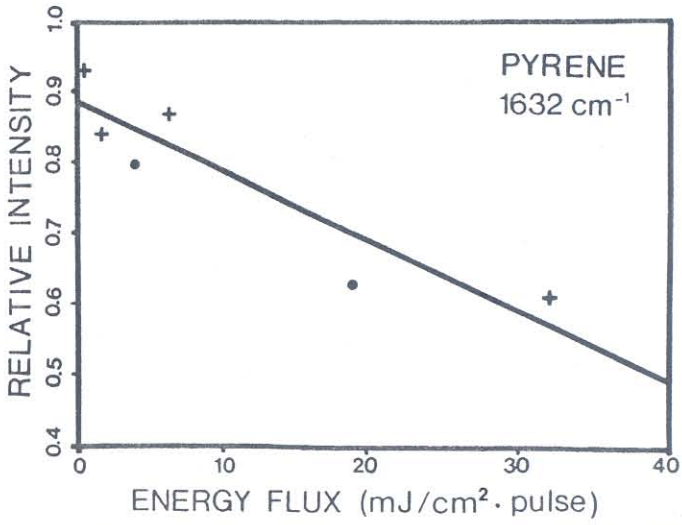

FIG. 5. The pulse energy flux dependence of the observed intensity ratio of the 1632 cm^{-1} band of pyrene relative to the 2249 cm^{-1} band of acetonitrile. The intensity data derive from Fig. 4, while the energy flux data derive from Table I. Note the lack of a linear dependence for the highest energy flux data not included in Fig. 5 from Fig. 4A and B (YAG). Excimer (+), YAG(●). The solid line shows the least-squares fit to the initial slope.

This improvement in signal-to-noise comes at a significant cost in equipment, ease of use, and cost of laser dyes. While the cost in terms of laser dye degradation has decreased somewhat, in comparison to the sums we estimated earlier,[25] it is still significant; in the experiments here, the cost ran to about $45/h. We are developing other techniques for upconverting the dye laser light into the UV to minimize the cost and inconvenience of excimer lasers. We are investigating multiple-order H_2 gas anti-Stokes Raman shifting, as well as using the new, high-efficiency β-BaB_2O_4 frequency-doubling crystals,[26,27] and will report on these efforts in the future.

CONCLUSIONS

The high peak powers which often accompany the use of nonlinear techniques for frequency upconversion can result in saturation and photochemical transient formation which can interfere with Raman spectral measurements. We demonstrate here that the use of a high-repetition-rate UV excimer pumped frequency-doubled dye laser (200 Hz, 16 ns pulses) avoids these optical phenomena and allows us to measure, for the first time, the absolute Raman cross sections of bands resonantly enhanced in the pyrene S_4 and tyrosinate S_2 electronic transitions. In addition, we demonstrate improved signal-to-noise ratios for spectra measured with the lower-energy-flux-per-pulse excimer-based UV excitation source.

ACKNOWLEDGMENTS

We gratefully acknowledge partial support of this work from NIH grant 1R01-GM30741-06. Sanford A. Asher is an Established Investigator of the American Heart Association; this work was done during the tenure of an Established Investigatorship of the American Heart Association and with funds contributed in part by the American Heart Association, Pennsylvania affiliate.

1. S. A. Asher, C. R. Johnson, and J. Murtaugh, Rev. Sci. Instrum. **54,** 1657 (1983).
2. B. Hudson, Spectroscopy **1(1),** 22 (1986).
3. L. D. Ziegler and C. Varotsis, Chem. Phys. Lett. **123,** 175 (1986).
4. B. S. Hudson, P. B. Kelley, L. D. Ziegler, D. P. Gerrity, R. A. Desiderio, R. Bates, and W. Hess, *Advances in Laser Spectroscopy,* B. A. Goretz and J. R. Lombardi, Eds. (Publisher, location, 1986), Vol. III, p. 1.
5. C. M. Jones, T. A. Naim, M. Ludwig, J. Murtaugh, P. Flaugh, J. M. Dudik, C. R. Johnson, and S. A. Asher, Trends Anal. Chem. **4,** 75 (1985).
6. L. D. Ziegler and B. S. Hudson, J. Chem. Phys. **79,** 1197 (1983).
7. J. M. Dudik, C. R. Johnson, and S. A. Asher, J. Chem. Phys. **82,** 1732 (1985).
8. C. R. Johnson, M. Ludwig, S. O'Donnell, and S. A. Asher, J. Am. Chem. Soc. **106,** 5008 (1984).
9. S. A. Asher, M. Ludwig, and C. R. Johnson, J. Am. Chem. Soc. **108,** 3186 (1986).
10. R. P. Rava and T. G. Spiro, J. Phys. Chem. **89,** 1856 (1985).
11. M. Ludwig and S. A. Asher, J. Am. Chem. Soc., in press (1987).
12. L. D. Ziegler, B. Hudson, D. P. Strommen, and W. L. Peticolas, Biopolymers **23,** 2067 (1984).
13. S. A. Asher, Anal. Chem. **56,** 720 (1984).
14. C. R. Johnson and S. A. Asher, Anal. Chem. **56,** 2258 (1984).
15. C. M. Jones and S. A. Asher, J. Am. Chem. Soc., in preparation (1987).
16. B. R. Stallard, P. M. Champion, P. R. Callis, and A. C. Albrecht, J. Chem. Phys. **78,** 712 (1983).
17. P. M. Champion and A. C. Albrecht, Ann. Rev. Phys. Chem. **33,** 353 (1982).
18. J. Teraoka, S. Alex, and S. A. Asher, Biochemistry, in preparation (1987).
19. M. D. Levenson, *Introduction to Nonlinear Laser Spectroscopy* (Academic Press, New York, 1982).
20. C. R. Johnson, M. Ludwig, and S. A. Asher, J. Am. Chem. Soc. **108,** 905 (1986).
21. D. Creed, Photochem. Photobiol. **39,** 563 (1984).
22. S. A. Asher, J. Teraoka, J. Am. Chem. Soc., in preparation.
23. C. R. Goldschmidt and M. Ottolenghi, J. Phys. Chem. **74,** 2041 (1970).
24. M. J. Sanders, R. S. Cooper, R. Jankowiak, V. Heisig, G. J. Small, and A. J. Jeffrey, Anal. Chem. **58,** 816 (1986).
25. S. A. Asher, Appl. Spectros. **38,** 276 (1984).
26. K. Kato, IEEE J. Quantum Electron. **QE-22,** 1013 (1986).
27. B. Hudson, Spectroscopy **2(4),** 33 (1987).

Phase-Modulation Fluorometry for On-Line Liquid Chromatographic Detection and Analysis of Mixtures of Benzo(k)fluoranthene and Benzo(b)fluoranthene

W. TYLER COBB* and LINDA B. McGOWN*†
Department of Chemistry, Oklahoma State University, Stillwater, Oklahoma 74078-0447

A phase-modulation fluorometer was used for on-line detection of benzo(k)fluoranthene and benzo(b)fluoranthene in a mixture of the two that was isocratically eluted from a high-performance liquid chromatographic column. Three different mobile-phase solvent compositions provided three degrees of chromatographic separation, ranging from complete to almost no separation. Fluorescence lifetimes were calculated from phase and modulation data that were collected at three different excitation modulation frequencies. Heterogeneity analysis was then used to calculate the fluorescence lifetimes and fractional intensity contributions of each component at each point along the chromatograms. The fractional intensity contributions were multiplied by the fluorescence intensities in the steady-state chromatogram of the mixture in order to construct the fluorescence intensity chromatograms of the individual components. Retention times and fluorescence lifetimes of the components obtained from the constructed chromatograms were in good agreement with values obtained from steady-state chromatograms of the individual components. Relative errors of the peak intensities were as high as 23%. Batch experiments were also performed to determine the best results that could be expected for the heterogeneity analysis of mixtures of the two components in the solvent systems that were used in the chromatographic experiments.

Index Headings: HPLC; Fluorescence detection for HPLC; Phase-modulation fluorescence detection; Phase-modulation fluorescence heterogeneity analysis.

INTRODUCTION

Multidimensional data formats have been used in fluorescence spectroscopy to provide highly selective determinations of fluorescent compounds in mixtures through the use of fluorescence spectral and lifetime information, as well as selective quenching and enhancement, linear and circular polarization, and other phenomena.[1,2] However, analysis of complex samples containing many fluorescent compounds will often require the use of a separation technique prior to the fluorimetric determinations; even then, the analyses of real samples may not be easily achieved.

Several approaches to the incorporation of on-line fluorescence lifetime determination into the fluorimetric detection of compounds eluted during high-performance liquid chromatography (HPLC) have been recently described, including the use of pulsed source laser excitation[3] and the use of phase-modulation fluorometry.[4] In the latter experiments, the apparent fluorescence lifetimes are calculated from the phase-shift and demodulation of the emission signal relative to the exciting light. The degree of agreement between the apparent phase and modulation lifetimes can be used as an indicator of chromatographic peak overlap, i.e., the presence of more than one fluorescent component at a given point along the chromatogram. Phase-modulation fluorescence chro-

Received 8 August 1987.
* Present address for both authors: Department of Chemistry, Gross Chemical Laboratory, Duke University, Durham, NC 27706.
† Author to whom correspondence should be sent.

0003-7028/87/4108-1275$2.00/0